

Interpreting the Passivation of HSLA Steel from Electrochemical Corrosion Investigations in Bicarbonate-Oil Aqueous Emulsions

Faysal Fayez Eliyan^{1*}, El-Sadig Mahdi², Zoheir Farhat³, Akram Alfantazi¹

¹Corrosion group, Department of Materials Engineering, The University of British Columbia, Vancouver, BC, Canada, V6T 1Z4

²Mechanical Engineering Department, College of Engineering, Qatar University, P.O. Box 2713, Doha, Qatar

³Department of Process Engineering and Applied Science, Dalhousie University, Halifax, NS, Canada, B3J 2X4

*E-mail: faysal09@interchange.ubc.ca

Received: 13 December 2012 / Accepted: 6 January 2013 / Published: 1 February 2013

This research proposes a schematic physical interpretation of passive films formed on HSLA steel during potentiodynamic polarization in bicarbonate-oil aqueous emulsions. The interpretation is based on the numerical calculation of charge-transfer release during the passivation process which showed an obvious disparity with bicarbonate and oil amounts. Other outcomes are attained with a primary objective to carrying out this research: the corrosion rates showed an increase with bicarbonate content and temperature, and oil acted as an anodic inhibitor. The EIS tests confirmed the corrosion inhibition and showed that the interfacial interactions that govern the corrosion reactions during the OCP conditions are adsorption-based.

Keywords: API-X100, oil, bicarbonate, polarization, EIS

1. INTRODUCTION

Multiphase corrosion stands as a main, common problem in the oil and gas transmission pipelines. The corrosion rates and natures depend on a wide matrix of interrelated variables such as temperature, total pressure, pH, salinity, dissolved gases, and flow rates and regimes [1-3]. From a chemistry perspective, the corrosion is primarily sustained by electroactive, carbon-carrying species of bicarbonate (HCO_3^-) and carbonate (CO_3^{2-}) in high-pH flows, and on carbonic acid (H_2CO_3) in low-pH ones [4-5]. This research specifically examines bicarbonate of different concentrations in driving the

corrosion reactions of a new pipeline steel API-X100 in deoxygenated solutions in the presence of an emulsified hydrocarbon. The solutions simulate mildly alkaline pipeline flows resulting after an excessive inhibitor injection or in the presence of “foreign” chemicals in situations that the dissolved CO₂ might eventually contribute to bicarbonate-governed reactions [6-7]. The direct reduction of bicarbonate is still of questionable significance [8-10], and yet investigating the roles of bicarbonate during the anodic and cathodic reactions and passivation in deoxygenated solutions/emulsions deserves more research efforts.

The polarization and other electrochemical methods were used by many researchers to study the corrosion of high-strength steels in bicarbonate solutions. Mao *et al.* reported that the corrosion rates of API-X80 increased and the polarization profiles changed with bicarbonate content [11]. Videm *et al.* studied the active-passive transition of Mn-Si microalloyed steel, reporting an effective passivation onset at -0.65 V vs. SCE in 0.1 and 0.5 M bicarbonate solutions during a 50 mV/min (0.833 mV/sec) polarization [12]. Torres-Islas *et al.* studied the polarization behavior of X-70 in dilute bicarbonate solutions of unbuffered 8.3 pH, reporting more noble passivation potentials (E_{pass}) with lessened bicarbonate content [13]. Li *et al.* and Mohorich *et al.* studied the effect of temperature on the corrosion of commercial pipeline steels in bicarbonate solutions of different chemistries [14, 15]. Their polarization results, whose profiles were similar, depicted a clear increase of the corrosion rates and passivation currents with temperature. Jelinek *et al.* studied the simultaneous effects of temperature and chloride on the passivation of microalloyed carbon steel in deoxygenated 0.1 M bicarbonate solutions, reporting a threshold 130 ppm chloride of passivation breakdown at 90°C [16]. In a similar work, the effects of the pH, chloride, and temperature were studied by Brossia *et al.* reporting some uncertainty on the corrosion rates and on the susceptibility of localized corrosion [17]. Alves *et al.* reported a two time-constant EIS response of the passivation developed on three carbon steels in 0.5 M bicarbonate solutions [18].

In the field, corrosion becomes, over time, much more susceptible when the amount of oil decreases and the amount of stratum water increases in flows transported from aging oil wells. Water-wetting surfaces increase to result in stable aqueous interfaces through which the corrosion reactions are accelerated. But if water content is low, the water phase is transported as entrained small droplets or dispersed slugs through the oil continuums where oil acts as an effective natural inhibitor [19]. However, the susceptibility for localized corrosion to proceed at high rates could depend on the water droplet size if the flow rates are low [20].

In literature, there is no well-established research on the corrosion behavior of pipeline steels in mildly alkaline flows that contain small amounts of crude oil. Instead, as we and Morales *et al.* previously reported, specific types of hydrocarbons were found effective in reducing the corrosion rates in CO₂-saturated solutions [21-22]. API-X100, a new high-strength steel of promising structural integrity, requires electrochemical studies in new laboratory conditions. Our results, in combination with other efforts, will be useful in effectively controlling the corrosive flows and understanding corrosion in real field situations.

In this research, we primarily aimed at investigating the effects of bicarbonate content, temperature, and oil on corrosion kinetics, passivation, and the possible OCP interactions on the corroding interfaces. From the disparities in the potentiodynamic passivation regimes, we proposed

schematics with which the roles of oil and bicarbonate into the final passivation structures could be approximately described. Moreover, both polarization and EIS results suggested that oil acts better as a natural inhibitor in the dilute solutions and at low temperatures.

2. EXPERIMENTAL

2.1. Corrosion test setup

The corrosion tests were performed in a standard three-electrode, 1-litre, glass jacketed cell. The working electrodes were made from API-X100 steel, the counter electrode was a graphite rod, and the reference electrode was the saturated calomel electrode (SCE). The ionic contact between the reference and working electrodes was maintained by a luggin capillary tube of a vycor frit close to the test surface. The jacketed chamber was connected by plastic tubes to a heating unit that circulates a constant-velocity water flow. A gas bubbler was placed inside the cell to purge argon to deoxygenate the solutions. A special valve was used to control the gas flow at an adequate cell pressure. The test emulsions were continuously stirred by a small magnetic bar to homogenize water and oil. The three electrodes were connected to PAR Versastat 4 potentiostat synchronized to VersaStudio software.

2.2. Test material

The test coupons were machined out of an API-X100 pipeline shell. They were soldered to copper wires by a conductive silver paste and mounted in hard epoxy resins. 120, 320, and 600-grit Silicon carbide papers were used to wet grind the corrosion samples. They were ultrasonically degreased with ethyl alcohol and rinsed with distilled water and dried in an air stream. The chemical composition analysis is shown in table 1.

Table 1. Chemical composition of the test material

Composition (wt. %)										C.E.
C	Mn	Mo	Ni	Al	Cu	Ti	Nb	Cr	V	
0.1	1.67	0.21	0.13	0.02	0.25	0.01	0.043	0.016	0.003	0.47

It was carried out by inductive coupled plasma (ICP) and LECO carbon analysis. The microstructure is shown in Fig. 1. It was studied from a sample, wet ground to 1200-grit silicon carbide finish and polished with 6 and 1 μm diamond suspensions. The sample was then immersed in a Nital etchant (2 mL of 70% nitric acid and 98 mL of anhydrous, denatured ethyl alcohol), treated with alcohol swapping, and dried in an air stream. The microstructure consisted of a mixture of ferrite and bainite of slight microvariations in colour.

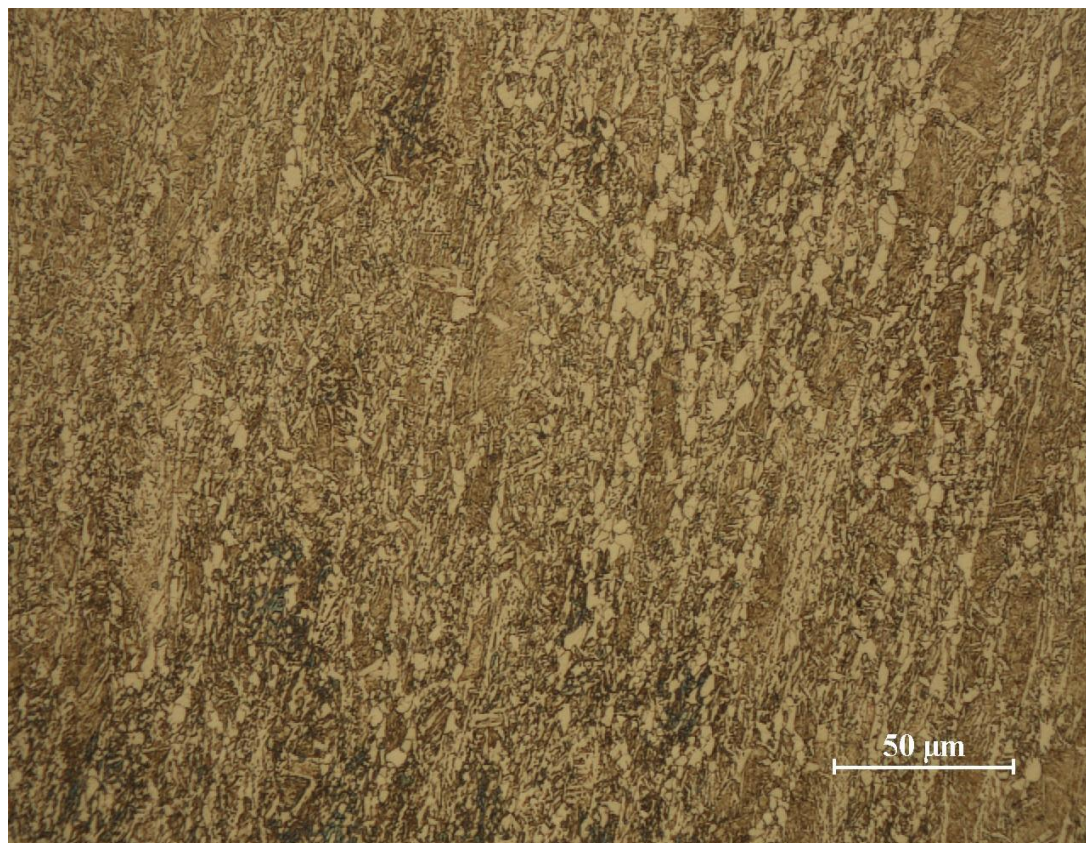


Figure 1. Optical micrograph of API-X100 microstructure

2.3. Test solutions

Table 2. Properties of the Shell© diesel fuel emulsified in bicarbonate test solutions

Property	Details
Appearance	Green
Carbon number	C4-C12
Initial Boiling Point (°C)	25
Boiling Range (°C)	25 - 170
Flash point (°C)	>10
Lower / upper Flammability (% V)	1 - 6
Auto-ignition temperature (°C)	> 250
Vapor pressure (kPa)	< 38 at 20 °C
Density (g/cm ³)	0.63 at 15 °C
Kinematic viscosity (mm ² /s)	0.5-0.75 at 40 °C

The deoxygenated solutions were synthesized from double-distilled, deionized water and 0.05, 0.1, 0.5, and 1 M bicarbonate and 30 ppm chloride. A hydrocarbon Shell© diesel fuel introduced with

10, 20, and 30 vol% was emulsified in the bicarbonate solutions with an anionic surfactant; dioctyl sulfosuccinate sodium ($C_{20}H_{37}NaO_7S$). It was introduced with a small amount of 0.2 wt% to homogenize the bicarbonate solutions with oil. The surfactant was successfully used by us [3], Quiroga Becerra *et al.*, and Zhang *et al.* [23, 24] in similar recent studies where the electrochemical tests were carried out in water-oil emulsions without reporting significant adsorption effects by the surfactant counteracting that of oil. Selected properties of the emulsified hydrocarbon are shown in table 2. They correspond, according to the classification criteria by Manning, to a special light crude oil [25]. The hydrocarbon consists of a complex mixture of paraffins, cycloparaffins, aromatic, and olefinic species. We proposed, in a different research, that 1-, 2-, 3-, 4-tetrahydronaphthalene ($C_{10}H_{12}$) could be responsible for corrosion suppression, sharing its π -electron density in a chemisorption fashion [26]. 30 and 70°C were the test temperatures maintained within $\pm 1^\circ\text{C}$.

2.4. Electrochemical tests

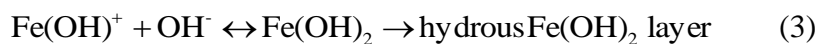
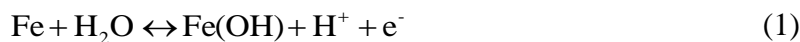
Before starting the experiments, a potentiostatic cathodic conditioning at -2 V vs. SCE was performed for 800 seconds right after immersing the samples in the test solutions. The experiments were repeated many times to ensure reproducibility. The potentiodynamic polarization was carried out with an upward 0.5 mV/sec scan. The cathodic polarization tests were carried out from -2 V vs. SCE to the corrosion potentials with the same scan rate and direction. The EIS tests were performed at the open circuit potentials from 10,000 to 0.01 Hz with a sampling rate of 10 points per decade.

3. RESULTS AND DISCUSSION

3.1 Potentiodynamic polarization

The potentiodynamic polarization at 30°C is shown in figure 2. Both in oil-free and oil-containing solutions, the anodic and cathodic current densities showed an increase with bicarbonate content and, more specifically, the corrosion rates increased, and the corrosion potentials decreased with bicarbonate content. Similar to results we and Parkins *et al.* reported from deoxygenated bicarbonate solutions, it suggests an active role of bicarbonate in catalyzing anodic dissolution [5] and [27]. The polarization behavior at 70°C was similar, but the corrosion rates were higher and the corrosion potentials were nobler.

The corrosion rates were between $120 \mu\text{A}/\text{cm}^2$ (1.4 mm/yr) and $208 \mu\text{A}/\text{cm}^2$ (2.41 mm/yr) at 30 and 70°C, respectively. These rates notably exceed the corrosion rates acceptable at high temperatures in oil pipelines that must be as low as 0.1 mm/year after pH stabilization [28]. Observable in the active regimes, the anodic currents showed inflections at about -0.88 V vs. SCE. That was associated to the formation of defective, semi-protective layers, reported previously by Valentini *et al.* and Castro *et al.* who carried out similar electrochemical studies in bicarbonate solutions [29, 30], mentioning the following mechanism:



$\text{Fe}(\text{OH})_2$, according to Niu *et al.*, can react with HCO_3^- (reaction 4) to result in an acceleration of the temporarily decelerated currents [31] as follows:

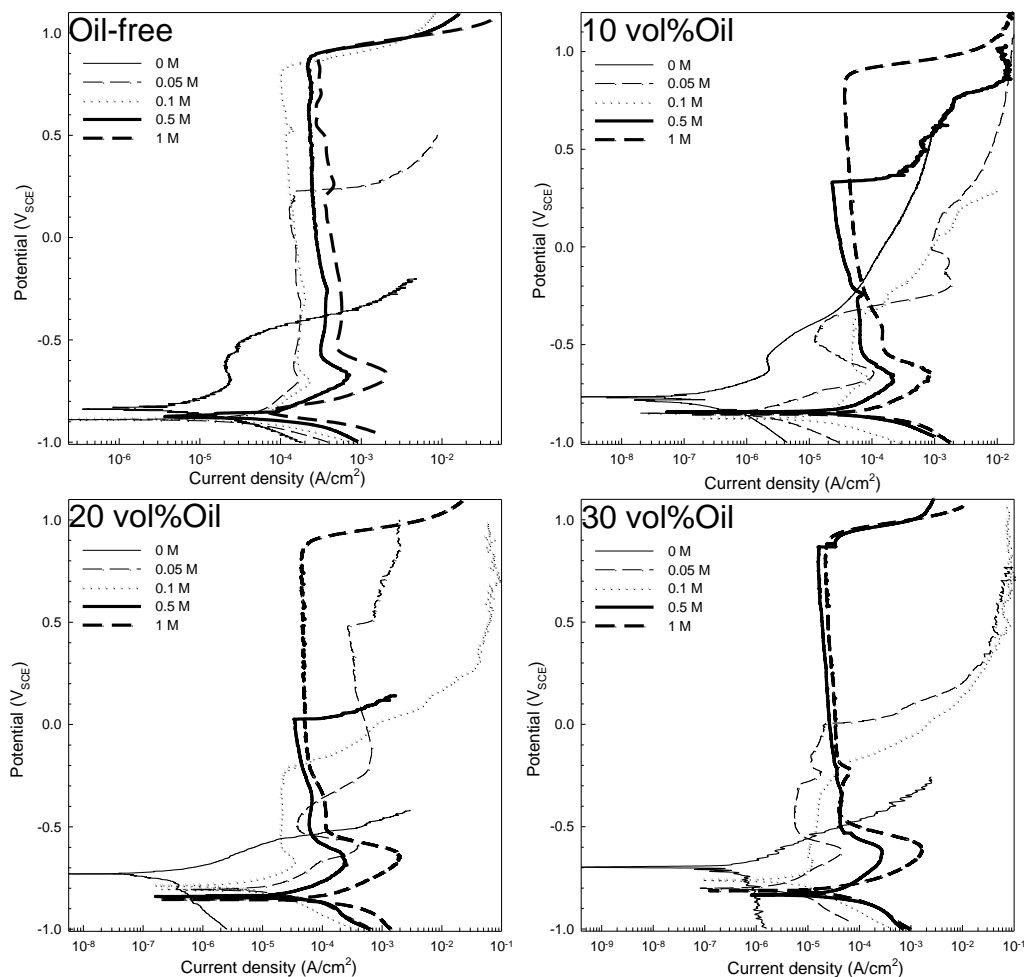


Figure 2. Potentiodynamic polarization at 30°C

The anodic peaks appeared at about -0.70 V vs. SCE with intensities relatively proportional with bicarbonate content. Simard *et al.* reported, from cyclic voltammograms of 1024 mild steel in bicarbonate solutions, that FeCO_3 precipitates during passivation reactions that involve bicarbonate and FeHCO_3^+ complexes [32]. Fe_3O_4 and Fe_2O_3 formation at the presence of FeCO_3 is possible but not to be mechanistically discussed in this research. Deodshemukh *et al.* reported from XPS and electrochemical tests that Fe_2O_3 can readily form as a result of FeCO_3 oxidation in bicarbonate

solutions [33]. Park *et al.* performed a similar work and also confirmed the presence of Fe_2O_3 in 0.5 M bicarbonate solutions [34]. Passivation current density (i_{pass}) was higher, and transpassivation seemed to commence at higher potentials, with bicarbonate content.

Oil, in a relatively proportional manner, reduced the current densities. Its effect seemed better in 0.05 and 0.1 M solutions (oil was more miscible in the dilute solutions). In most cases, the corrosion potentials were higher than in the oil-free solutions, suggesting an anodic inhibition effect [35]. Oil, moreover, delayed the onset of effective passivation in a situation the solubilities of the corrosion species have possibly changed at the emulsified interfaces [36]. Passivation in 0.05 and 0.1 M solutions was notably disrupted as depicted from the potential-current passivation regimes. Passivation current density, independent from bicarbonate content, was less than the oil-free solutions. This suggests that oil might have inhibited certain transport processes or preserved stable physical adsorption locations on/within the passive films. Such suggestions arose from our visual observations, but they indeed require innovated experimental methods with which the interactions between the passive films and any organic agents can be more precisely described. Increasing the oil content seemed to delay transpassivation to occur at higher potentials and passivation to be of fewer disruptions. Oil at 70°C decreased the corrosion rates, and its interactions with passivation seemed relatively similar to the 30°C conditions.

Charge transfer release during passivation was numerically calculated, from which the possible physical role(s) of oil during passivation could be visualized. In 0.05 M solutions at 30°C, as shown in figure 3a, the charge transfer release was high where oil was probably most effective to adsorb on the surface and/or disrupt passivation.

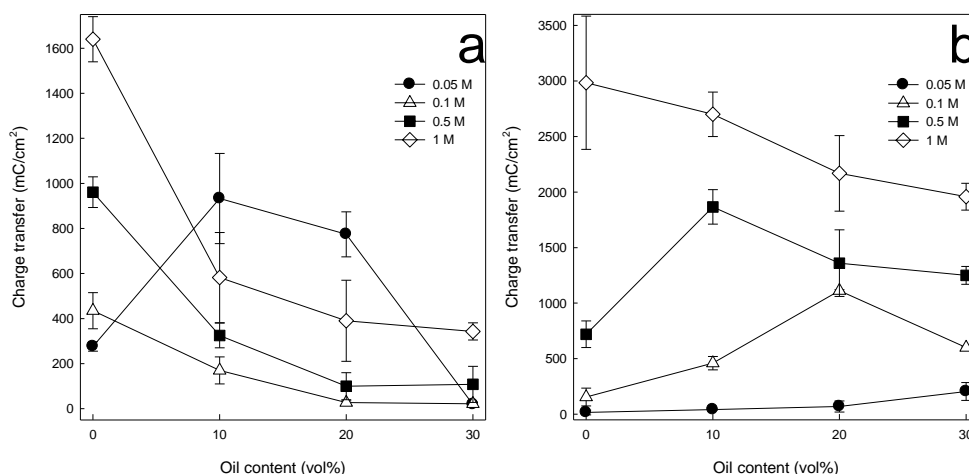


Figure 3. Passivation charge transfer at a) 30, and b) 70°C

Increasing oil content, however, decreased the charge transfer where passivation, to a limited, unknown extent, could have become oil-rich. Charge transfer showed a decrease with oil content in 0.1, 0.5, and 1 M solutions for reasons possibly still valid to propose from the 0.05 M cases, except that passivation could be assumed thicker. The schematics in figure 4 represent the possible interfaces of passivation in the presence of oil. Charge transfer density at 70°C was higher and it seemed to

decrease with oil content. It should be noted that passivation regimes and charge transfer cannot be the only sources of knowing the physical state of developing passivation, so other combined methods should be used with physical characterization of passive films to grow during longer term experiments.

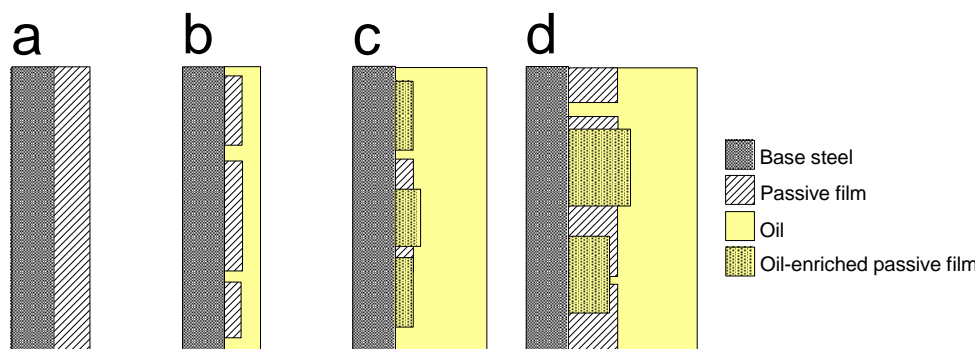


Figure 4. Proposed passivation interfaces in a) oil-free, b) 10 vol% oil, c) 30 vol% oil and d) bicarbonate-concentrated 30 vol% oil solutions

The cathodic polarization from $-2 V_{SCE}$ to the corrosion potentials at 30 and 70°C is shown in figure 5, where the current densities seemed mostly proportional with bicarbonate content. Oil decelerated the current densities, more notably during the mass-limited reduction, possibly suggesting less permeability of bicarbonate and other reduced species through the emulsified interfaces.

3.2 Electrochemical impedance spectroscopy

EIS was performed to study the interfacial interactions in the open circuit potential conditions. The impedance was fitted with equivalent circuits to study charge transfer and transport across specific interfaces with elements like charge transfer resistance (R_{ct}), double layer capacitance (C_{dl}), and Warburg element (W) [37]. The EIS response in oil-free conditions at 30°C is shown figure 6. The Nyquist spectra were similar but the greatest size of 0.05 M reflected a high charge transfer resistance, showing an agreement with the polarization's minimum corrosion rates in 0.05 M solutions.

The profiles mainly consisted of two overlapped capacitive loops, more apparent in the concentrated solutions at about 0.25 Hz, representing adsorption-governed processes [38]. Adsorption could mainly be governed by the intermediate $[FeHCO_3^-]_{ads}$, $[FeHCO_3^+]_{ads}$, and $[FeOH]_{ads}$ species, but its dependence on bicarbonate content and/or its rate-determining steps that involve some of the intermediates are difficult to determine. The impedance modules $|Z|$ depicted a clear dependence of EIS on bicarbonate content in the high- and low-frequency regions; i.e. bicarbonate, regardless of the content, could have simultaneously affected charge transfer and adsorption. The phase profiles were similar and sole phase peaks appeared between 10 and 50 Hz. The proposed equivalent circuit $\{R(Q(R(QR)))\}$, shown in figure 7, achieved a good fitting with the experimental data. Other

equivalent circuits proposed by Li *et al.* and others [14, 18], for EIS in bicarbonate solutions, were attempted.

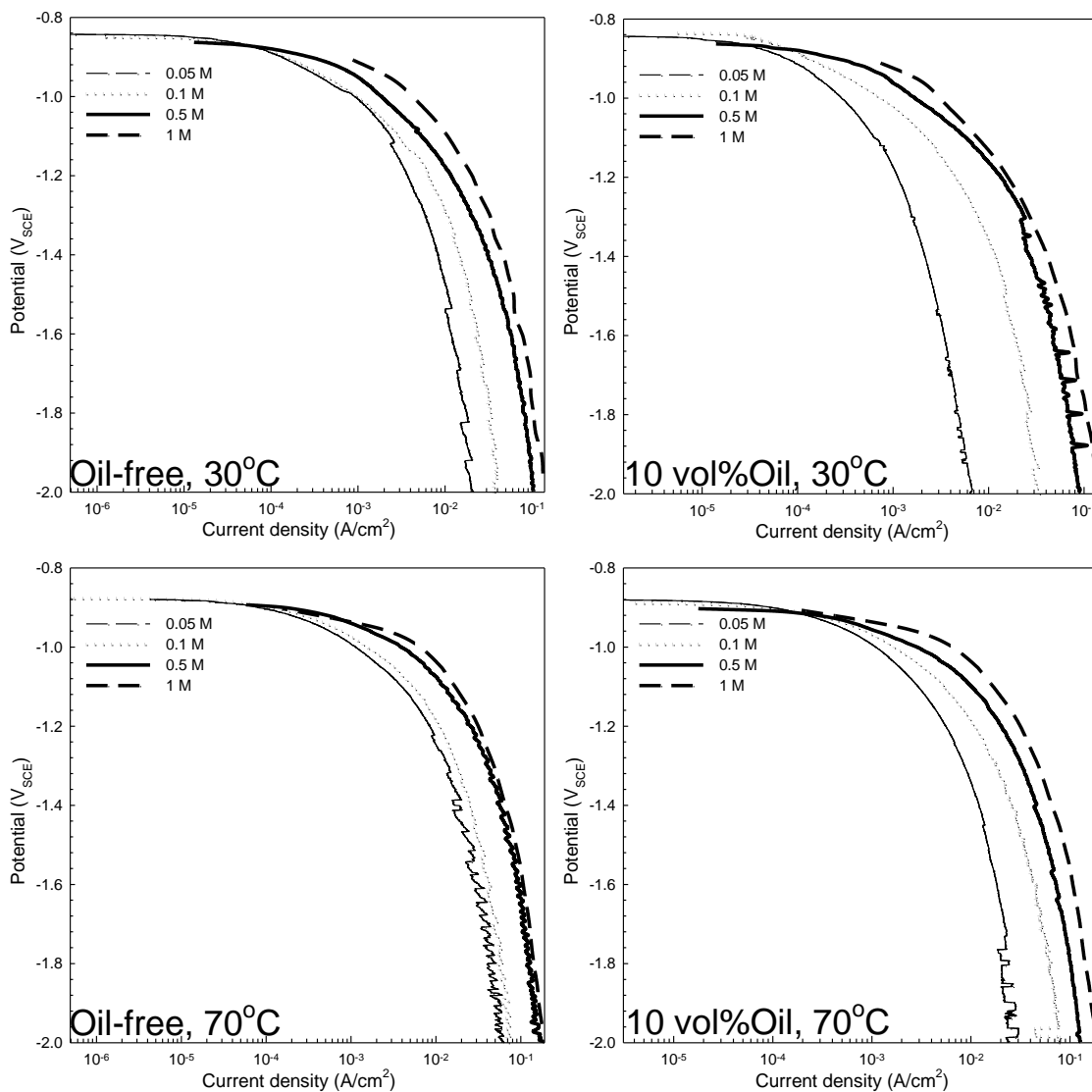


Figure 5. Cathodic polarization at 30 and 70°C

They were not suitable to represent the low-frequency, double-layer processes in our cases. A constant phase element (CPE) was considered to account for interfacial heterogeneities:

$$Z_{CPE} = [Q(j\omega)^n]^{-1} \quad (5)$$

The resistances of charge transfer and adsorption decreased with bicarbonate content and their interfaces were capacitive. Depicted from oil-containing conditions, shown in figure 8 at 30°C, oil seemed to affect EIS response most in the dilute solutions where oil was more miscible and the emulsified interfaces were more stable.

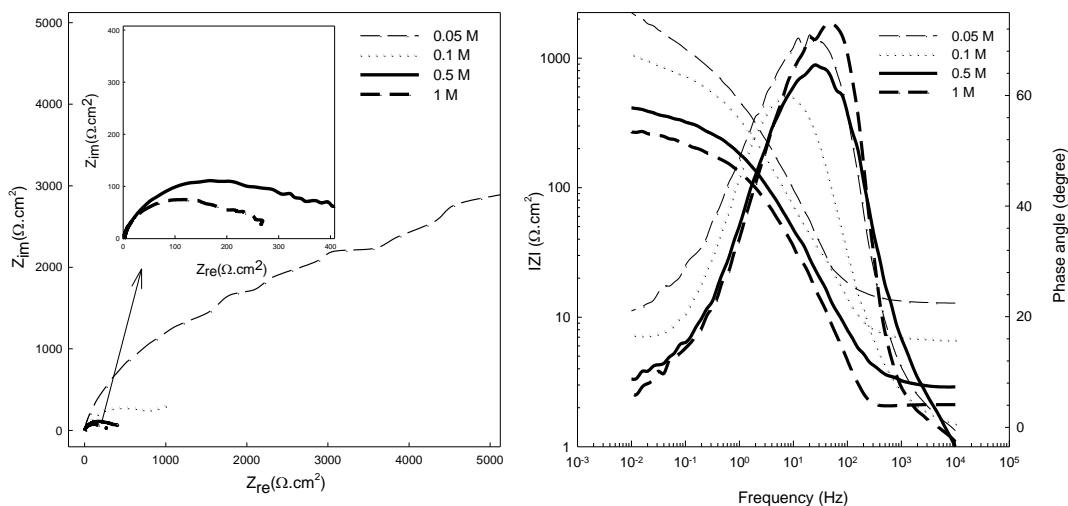


Figure 6. Nyquist and Bode EIS in oil-free solutions at 30°C

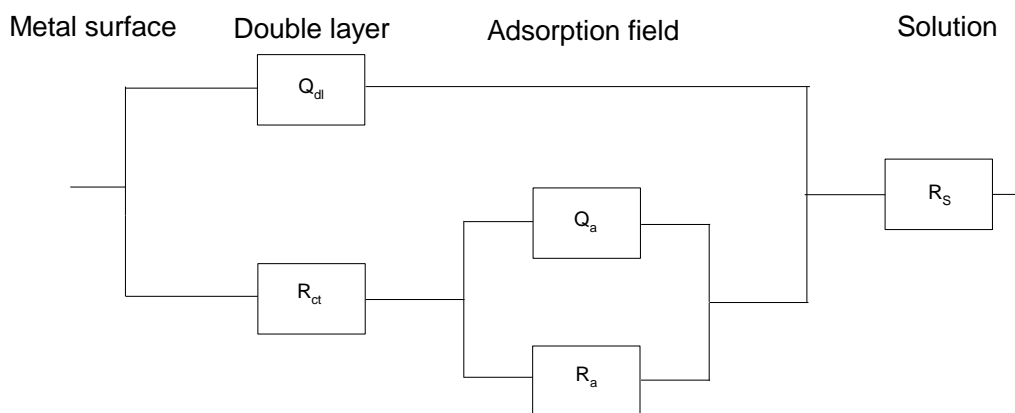


Figure 7. The equivalent circuit for EIS in oil-free conditions

EIS behavior was similar to that reported by Chen *et al.* in CO₂-saturated multiphase flows [2]. This might suggest that the corroding steels’ interactions in CO₂-saturated and bicarbonate solutions could be dependent on intermediate, carbon-carrying adsorbents regardless of pH and/or flow at the presence of oil. Both Nyquist and Bode spectra, in general, depicted a multi-time-constant EIS in 0.05 M solutions. An equivalent circuit was attempted to fit 0.05 M solutions’ EIS on the assumption that oil could adsorb on stable passive films. {R(CR)(QR)} and {R(QR)(QR)} circuits did not achieve a good fitting but {R(QR)(QR)(QR)}, shown in figure 9, reliably did. Charge transfer resistance notably increased upon the introduction of oil. The EIS, outside the double layer, was capacitive for reasons difficult to explain but similar to that reported by Lopez *et al.* who studied CO₂ corrosion in the presence of two commercial imidazoline-based inhibitors [39]. EIS in 0.1 M, oil-containing solutions was well-fitted with a two time-constant circuit with a Warburg element (W). EIS, regardless of oil content, in 0.5 and 1 M solutions seemed similar to the oil-free conditions’ where oil was less miscible.

EIS at 70°C was similar to the 30°C oil-free and oil-containing conditions' but the Nyquist spectra were smaller, and the charge, adsorption, and solution resistances were remarkably less.

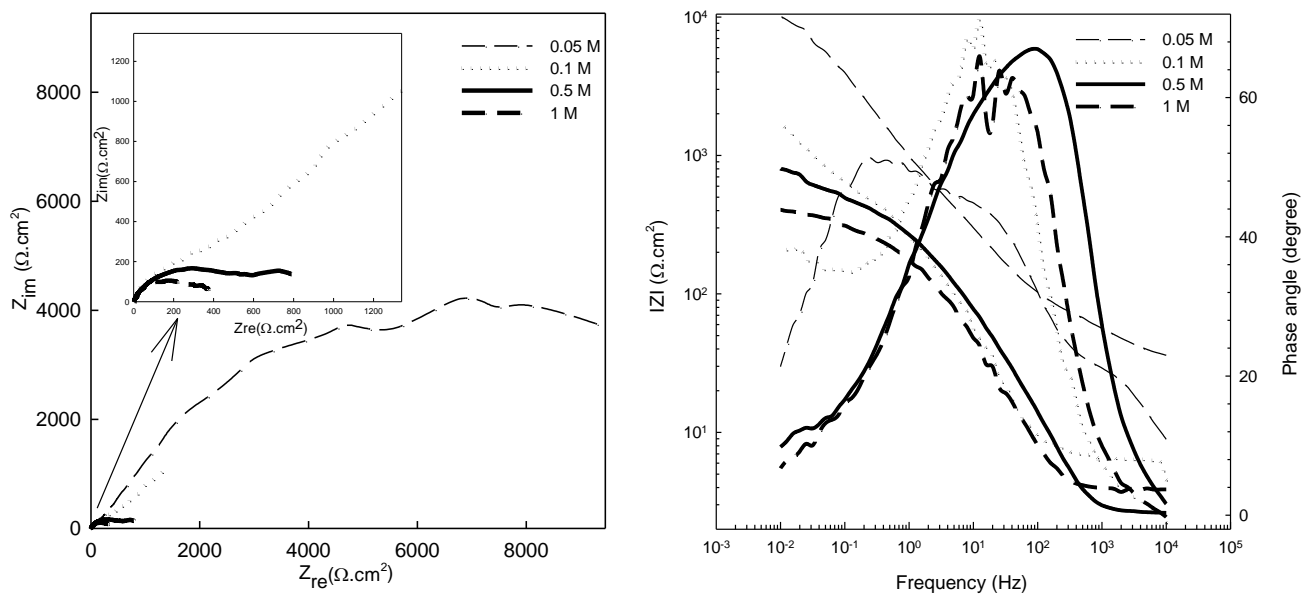


Figure 8. Nyquist and Bode EIS in 10 vol%-oil-containing solutions at 30°C

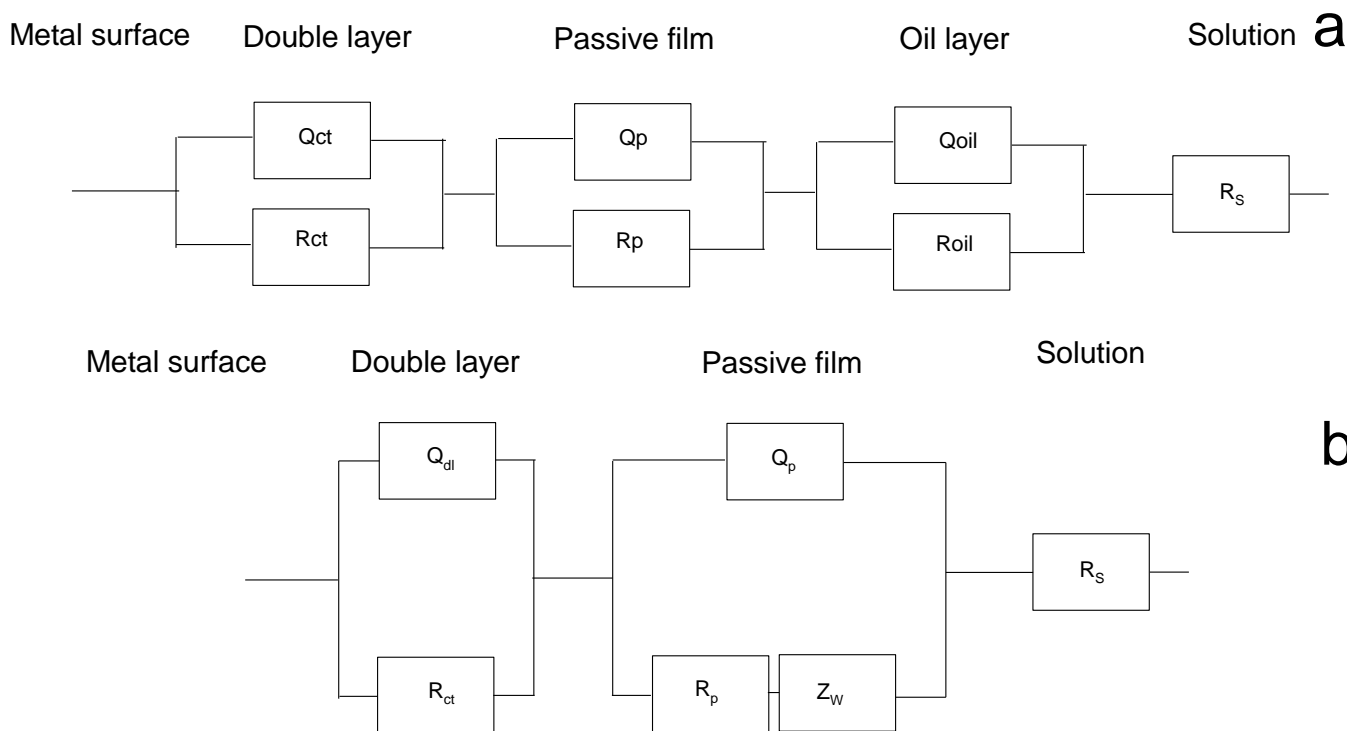


Figure 9. The equivalent circuits for EIS in oil-containing a) 0.05 M and b) 0.1 M bicarbonate solutions

4. CONCLUSIONS

The corrosion rates and selected aspects in kinetics, passivation, and EIS of API-X100 corrosion were studied in special bicarbonate solutions. The effects of bicarbonate and oil contents were investigated at 30 and 70°C in deoxygenated, continuously-stirred emulsions. The corrosion rates increased with bicarbonate content and temperature. The passivation potential ranges were broad, showing single anodic peaks at comparable potentials and with intensities relatively dependent on bicarbonate content. Oil decelerated the current densities and, therefore, the corrosion rates, and disrupted passivation in a fashion from which possible passivation interfaces in the presence of oil were proposed. The EIS response of oil-free conditions depicted adsorption-controlled interactions, while it seemed multi-time-constant based in the emulsions. There was good agreement between the polarization and EIS results.

ACKNOWLEDGEMENTS

This publication was made possible by NPRP grant # 09-211-2-089 from the Qatar National Research Fund (a member of Qatar Foundation). The statements made herein are solely the responsibility of the authors.

References

1. G. Ogundele and W. White, *Corrosion*, 43 (1987) 665.
2. Y. Chen, *Electrochim. Acta*, 44 (1999) 4453.
3. F. Eliyan, F. Mohammadi and A. Alfantazi, *Corros. Sci.*, 64 (2012) 37.
4. S. Nestic, *Corros. Sci.*, 49 (2007), 4308.
5. R. Parkins and S. Zhou, *Corros. Sci.*, 39 (1997) 175.
6. W. Lyons and G. Plisga, *Standard handbook of petroleum & natural gas engineering*, Elsevier, London (2005).
7. K. Videm, Fundamental studies aimed at improving models for prediction of CO₂ corrosion, in: *Proceedings from 10th European Corrosion Congress, Progress in the Understanding and Prevention of Corrosion*, vol. 1. (London: Institute of Metals, 1993), p. 513.
8. F. Eliyan, E. Mahdi and A. Alfantazi, *Corros. Sci.*, 58 (2012) 181.
9. F. Mohammadi, F. Eliyan and A. Alfantazi, Corrosion of simulated weld HAZ of API X-80 pipeline steel, *Corros. Sci.*, 63 (2012) 323.
10. L. Gray, B. Anderson, M. Danysh and P. Tremaine, Effect of pH and temperature on the mechanism of carbon steel corrosion by aqueous carbon dioxide, *CORROSION/1990*, NACE International, Houston, TX, 1990, paper 40.
11. X. Mao, X. Liu and R. Revie, *Corrosion*, 50 (1994) 651.
12. K. Videm and A. Koren, *Corrosion*, 49 (1993) 746.
13. A. Torres-Islas, J. Gonzalez-Rodriguez, J. Uruchurtu and S. Serna, *Corros. Sci.*, 50 (2008) 2831.
14. J. Li and J. Zuo, *Chin. J. Chem.*, 26 (2008) 1799.
15. M. Mohorich, J. Lamb, D. Chandra, J. Daemen and R. Rebak, *Metal. and Mtrl. Transc. A*, 41 (2010) 2563.
16. J. Jelinek and P. Neufeld, *Corros. Sci.*, 20 (1980) 489.
17. C. Brossia and G. Cragnolino, *Corrosion*, 56 (2000) 505.
18. V. Alves and C. Brett, *Electrochim. Acta*, 47 (2002) 2081.

19. U. Lotz, L. van Bodegom and C. Ouwehand, The effect of type of oil and gas condensate on carbonic acid corrosion, CORROSION/1990, NACE International, Houston, TX, 1990, paper 41.
20. J. Smart, Wettability – A major factor in oil and gas system corrosion, CORROSION/1993, NACE International, Houston, TX, 1993, paper 70.
21. F. Eliyan and A. Alfantazi, *J. Appl. Electrochem.*, 42 (2012) 233.
22. J. Morales, J. Perdomo, M. Ramirez and A. Vilorio, Effect of crude oil contaminations on the internal corrosion in gas pipelines, CORROSION/2000, NACE International, Houston, TX, 2000, paper 40.
23. H. Quiroga Becerra, C. Retamoso and D. Macdonald, The corrosion of carbon steel in oil-in-water emulsions under controlled hydrodynamic conditions, *Corros. Sci.*, 42 (2000) 561.
24. G. Zhang and Y. Cheng, *Corros. Sci.*, 51 (2009) 901.
25. F. Manning and R. Thompson, *Oilfield Processing of Petroleum: Crude oil*, PennWell publishing Co., Oklahoma (1995).
26. F. Eliyan and A. Alfantazi, Adsorption of oil, and effects of temperature and chloride ions on the corrosion behavior of API-X100 pipeline steel in CO₂-saturated solutions, *Metall. Mater. Trans. B*, (2012) Under Review.
27. F. Eliyan and A. Alfantazi, Electrochemical evaluation of the corrosion behavior of API-X100 pipeline steel in 1-bar CO₂-HCO₃⁻ solutions, *Mater. Chem. Phys.*, (2012), Under Review.
28. R. Nyborg, *Controlling Internal Corrosion in Oil and Gas Pipelines*, Oil and Gas Review (Issue 2) (2005).
29. C. Valentini and C. Moina, *Corros. Sci.*, 25 (1985) 985.
30. E. Castro, C. Valentini, C. Moina, J. Vilche and A. Arvia, *Corros. Sci.*, 26 (1986) 781.
31. L. Niu and Y. Cheng, *Appl. Surf. Sci.*, 253 (2007) 8626.
32. S. Simard, M. Drogowska and H. Menard, *J. Appl. Electrochem.*, 27 (1997) 317.
33. V. Deodeshmukh, A. Venugopal, D. Chandra, A. Yilmaz, J. Daemen, D. Jones, S. Lea and M. Engelhard, *Corros. Sci.*, 46 (2004) 2629.
34. J. Park, S. Pyun, W. Lee and H. Kim, *Corrosion*, 55 (1999) 380.
35. C. Mendez, S. Duplat, S. Hernandez and J. Vera, “On the mechanism of corrosion inhibition by crude oils”, CORROSION/2001, NACE International, Houston, TX, 2001, paper 1044.
36. M. Castillo, H. Rincon, S. Duplat, J. Vera and E. Baron, “Protective properties of crude oils in CO₂ and H₂S corrosion”, CORROSION/2000, NACE International, Houston, TX, 2000, paper 5.
37. R. Cottis, S. Turgoose and B. Syrett, *Corrosion Testing Made Easy: Electrochemical Impedance and Noise*, 1st ed. NACE, Houston, 1999.
38. H. Ma, X. Cheng, S. Chen, C. Wang, J. Zhang and H. Yang, *J. Electroanalyt. Chem.*, 451 (1998) 11.
39. D. Lopez, S. Simison and S. de Sanchez, *Corros. Sci.*, 47 (2005) 735.